

1 **The simultaneous insertion of two ligands in gD for the cultivation of oncolytic HSVs in non-**
2 **cancer cells and the retargeting to cancer receptors**

3

4

5

6 Valerio Leoni^{1*}, Biljana Petrovic^{1,2*}, Tatiana Gianni¹, Valentina Gatta^{1§}, Gabriella Campadelli-
7 Fiume^{1§}

8

9

10

11 ¹Department of Experimental, Diagnostic and Specialty Medicine, University of Bologna, Bologna,
12 Italy.

13

14

15

16

17

18

19

20

21

22

23

24

25

26

27

28

29

30

31

32

33

34

35

36

37

38

39

40

41

42

¹Department of Experimental, Diagnostic and Specialty Medicine, University of Bologna, Bologna,
Italy.

²Nouscom SRL, Rome, Italy

Running Head: Double gD retargeting

§ Corresponding authors:

Gabriella Campadelli-Fiume

Department of Experimental, Diagnostic and Specialty Medicine

University of Bologna

Via San Giacomo, 12

40126 Bologna, Italy

tel +39 051 2094733/34

FAX +39 051 2094735

email: gabriella.campadelli@unibo.it

Valentina Gatta

Department of Experimental, Diagnostic and Specialty Medicine

University of Bologna

Via San Giacomo, 12

40126 Bologna, Italy

email: valentina.gatta6@unibo.it

* contributed equally to this work

KEYWORDS. HER2, HSV, retargeting, gD, Vero, oncolytic virus

43 **ABSTRACT**

44 Insertion of a single chain antibody (scFv) to HER2 (human epidermal growth factor receptor 2) in
45 gD, gH, or gB gives rise to herpes simplex viruses (HSVs) specifically retargeted to HER2-positive
46 cancer cells, hence in highly specific non-attenuated oncolytic agents. Clinical grade virus
47 production can not rely on cancer cells. Recently, we developed a double retargeting strategy
48 whereby gH carries the GCN4 peptide for retargeting to the non-cancer producer Vero-GCN4R cell
49 line, and gD carries the scFv to HER2 for cancer retargeting. Here, we engineered double retargeted
50 recombinants, which carry both the GCN4 peptide and the scFv to HER2 in gD. Novel, more
51 advantageous detargeting strategies were devised, so as to optimize the cultivation of the double-
52 retargeted recombinants. Nectin1 detargeting was achieved by deletion of aa 35-39, 214-223, or
53 219-223, and replacement of the deleted sequences with one of the two ligands. The latter two
54 deletions were not attempted before. All recombinants exhibited the double retargeting to HER2
55 and to the Vero-GCN4R cells, as well as detargeting from the natural receptors HVEM and nectin1.
56 Of note, some recombinants grew to higher yields than others. The best performing recombinants
57 carried a gD deletion as small as 5 amino acids, and grew to titers similar to those exhibited by the
58 singly retargeted R-LM113, and by the non-retargeted R-LM5. This study shows that double
59 retargeting through insertion of two ligands in gD is feasible and, when combined with appropriate
60 detargeting modifications, can result in recombinants highly effective *in vitro* and *in vivo*.

61

62

63 **IMPORTANCE**

64 There is increasing interest in oncolytic viruses, following FDA and EMA approval of the oncolytic
65 HSV Oncovex^{GM-CSF}, and, mainly, because they greatly boost the immune response to the tumor
66 and can be combined with immunotherapeutic agents, particularly immune checkpoint inhibitors. A
67 strategy to gain high cancer specificity and avoid virus attenuation is to retarget the virus tropism to
68 cancer-specific receptors of choice. However, cultivation of retargeted oncolytics in cells
69 expressing the cancer receptor may not be approvable by regulatory agencies. We devised a strategy

70 for their cultivation in non-cancer cells. Here, we describe a double retargeting strategy, based on
71 the simultaneous insertion of two ligands in gD, one for retargeting to a producer, universal Vero
72 cell derivative, one for retargeting to the HER2 cancer receptor. These insertions were combined
73 with novel, minimally-disadvantageous detargeting modifications. The current and accompanying
74 studies teach how to best achieve the clinical-grade cultivation of retargeted oncolytics.
75

76 INTRODUCTION

77 Oncolytic viruses have come of age (1-5) since the approval by FDA and EMA of an oncolytic
78 herpes simplex virus (HSV), initially named Oncovex^{GM-CSF} or T-Vec, for the treatment of
79 metastatic melanoma (6, 7). Several generations of oncolytic HSVs were designed and tested in
80 preclinical assays and in clinical trials. Many of them achieve cancer specificity by virtue of
81 attenuation, frequently obtained through the deletion of the $\gamma_134.5$ gene, whose product counteracts
82 the IFN and PKR response of the cell to the virus (7-10). In other examples, additional genes were
83 deleted (11, 12). The resulting recombinants exhibited varying degrees of attenuation. A drawback
84 of attenuation is that not all cancer cells sustain a robust replication of these viruses.

85 An alternative strategy to attenuation has been to obtain cancer specificity through the
86 modification of the HSV tropism and tropism retargeting to a cancer specific receptor of choice,
87 coupled with detargeting from natural receptors (13-21). In our laboratory the targeted cancer
88 receptor is HER2 (human epidermal growth factor receptor 2), expressed in breast, ovary, stomach,
89 lung and other cancers (22). While the HER2-positive cancers are usually treated with anti-HER2
90 monoclonal antibodies, exemplified by trastuzumab and pertuzumab, only a fraction of cancers is
91 sensitive to this treatment, and resistance develops frequently (23).

92 HSV enters cells through the concerted action of four envelope glycoproteins, named gD,
93 gH/gL and gB, which are activated in a cascade fashion by interaction with cognate receptors and
94 intermolecular signaling (24-29). Briefly, gD interacts alternatively with HVEM or nectin1 (30-32).
95 The receptor-bound gD activates gH/gL, which is additionally activated by $\alpha v\beta 6$ or $\alpha v\beta 8$ -integrins
96 (33, 34). gH activation results in the displacement of gL (35), and is then transmitted to gB, which
97 executes the fusion between the virion envelope and the cell membrane (36). In the retargeted
98 viruses, a new ligand, exemplified by a single chain antibody to HER2, is engineered in gD, in gH,
99 or in gB, while appropriate deletions in gD ensure the detargeting from gD natural receptors (13,
100 15-17, 37, 38). The chimeric glycoproteins which carry the scFv to HER2 mediate HSV entry

101 through HER2. Because of the detargeting-retargeting these oncolytic HSVs strictly depend on
102 HER2 for infection.

103 For clinical grade preparations of retargeted oncolytic HSVs, it is advisable to avoid the
104 virus cultivation in HER2-positive cancer cells. To meet these needs, we recently developed a
105 system for the cultivation in non-cancer cells of HSVs retargeted to HER2, and, potentially, to any
106 cancer-specific receptor of choice. The system is based on a double retargeting strategy. One
107 retargeting is to the HER2, or any cancer receptor of choice. The other retargeting is by way of the
108 20 aa long GCN4 peptide, which readdresses the tropism to Vero cells expressing the artificial
109 receptor named GCN4R (39). The latter is made by a single chain antibody to GCN4 (40) fused to
110 domains II, III, TM and C tail of nectin1. The choice of the Vero cells as recipients of GCN4R
111 rested on the notion that wt-Vero cells have been approved by FDA for the clinical grade
112 preparations of Oncovex^{GM-CSF} (commercial name Imlygic), the derivative named Vero-His is
113 approved for clinical grade preparations of oncolytic Measles viruses (41), and, more generally, wt
114 Vero are approved for growth of a number human vaccines. The R-213 recombinant was
115 readdressed to GCN4R by engineering the GCN4 peptide in gH; simultaneously, it was readdressed
116 to HER2 by insertion of the scFv to HER2 in gD, in place of aa 6-38 (39). This deletion detargets
117 HSV tropism from HVEM and nectin1 (17).

118 The aims of this work were two-fold. First, to explore alternative ways to co-express the
119 scFv to HER2 for cancer retargeting and the GCN4 peptide for *in vitro* cultivation in the Vero-
120 GCN4R cells. Second, to define novel, less disadvantageous detargeting strategies, so as to
121 optimize the cultivation of retargeted oncolytic HSVs in the non-cancer cells.

122

123

124 **RESULTS**

125 **Double gD retargeting and novel detargeting.** An aim of this work was to ascertain whether gD
126 can simultaneously accept two retargeting moieties, the GCN4 peptide and the scFv to HER2. To

127 better accomplish this task, we reduced the size of the deletion in gD, so as to maintain the
128 detargeted phenotype, and preserve gD sequences, and possibly gD structure, as much as possible.
129 Our initial gD detargeted/retargeted viruses R-LM113 and R-LM249, which carry the deletion of aa
130 6-38, or 61-218 (17, 19), respectively, were designed at times when the regions of interaction
131 between gD and its receptors were known mainly through molecular biology approaches, and
132 through structural information on HVEM-bound gD (32). Indeed, the deletion of aa 38 in R-LM113
133 preceded the detailed knowledge of the nectin1 binding site in gD. Here, we took advantage of the
134 information on gD contact area with nectin1, inferred from the structure of gD bound to nectin1, as
135 determined by x-ray crystallography (42). According to the co-crystal structure, a tip in nectin1
136 protrudes into a groove in gD, whose critical residues include the previously known Y38 and the
137 adjacent residues, including H39, and residues 215 and 220-223. Those structural studies suggested
138 two alternative possibilities for nectin1 detargeting. One was the deletion of aa 35-39. The other
139 was the deletion of the region which includes aa 214-223 (42), not assayed before in detargeting
140 studies. Here we removed aa 214-223, or 219-223. The HVEM detargeting was achieved by the
141 simple insertion of the GCN4 peptide or of the scFv to HER2 between aa residues 24 and 25, which
142 are part of the HVEM binding site (32).

143 The list of double-insertion gD recombinants is reported in Table 1, which also summarizes
144 essential phenotypic features of the recombinants. The genome backbone is shown in Fig. 1 A. The
145 specific genotypes are shown in Fig. 1 B. The tropism was assayed in the HER2-positive cancer
146 cells SK-OV-3, in wt-Vero cells and in Vero-GCN4R, which express the artificial receptor to
147 GCN4 peptide (39) and in J cells derivatives. J cells express no receptor for HSV; derivatives
148 expressing a single receptor - HER2, nectin1, HVEM - were described (16, 43). R-LM113,
149 retargeted to HER2 but not to GCN4R, was included as control. The tropism of R-87, R-89, R-97,
150 R-99, R-99-2 is shown in Fig. 2, A-F. Cumulatively, the results show the following. (i) All
151 recombinants were detargeted from HVEM and from nectin1, since they failed to infect J-nectin1
152 and J-HVEM cells. (ii) All recombinants were retargeted to HER2, as inferred by the infection of J-

153 HER2 and SK-OV-3 cells, and by inhibition of infection by trastuzumab, the MAb to HER2 from
154 which the scFv employed for retargeting was derived (44). This property is shared with R-LM113.
155 (iii) All recombinants, except R-89, infected wt-Vero cells. This infection was inhibited by
156 trastuzumab, hence most likely it occurred through the simian ortholog of hHER2. The genome
157 sequence of Vero cell is incomplete, and, so far, there is no documentation of a HER2 homologue.
158 However, Vero cells were isolated from an Africa Green Monkey (*Chlorocebus* sp.), and the
159 sequence of the *Chlorocebus* genome contains the HER2 homologue (*Chlorocebus sabaues*;
160 REFSEQ: XM_008012845.1) with 98% identity with the human HER2 at the amino acid level. (iv)
161 All recombinants infected Vero-GCN4R cells. This infection was only in part decreased by
162 trastuzumab, indicating that it occurred in part through the GCN4 peptide present in the
163 recombinants, and its interaction with the GCN4R. (v) There was no difference in the recombinant
164 tropism whether the viruses were grown in Vero-GCN4R or in SK-OV-3 cells, as exemplified for
165 R-87 and R-99 (Fig. 2 G-H). Altogether, the results indicate that double retargeting through the
166 insertion of two different retargeting moieties in gD is feasible. All three nectin1-detargeting
167 strategies based on $\Delta 35-39$, $\Delta 214-223$, or $\Delta 219-223$ were effective. The detargeting through
168 deletion of the 214-223 or 219-223 regions were not attempted before.

169 **Comparative growth of double gD-retargeted recombinants.** We compared the yield of
170 the above recombinants to those of the wt HSV-1(F), the wt-gD recombinant named R-LM5, and
171 the singly HER2-retargeted R-LM113, in SK-OV-3 and in Vero-GCN4R cells. R-LM5 carries a wt-
172 gD, the BAC plus EGFP sequences, and is therefore the wt counterpart of the retargeted HSVs. A
173 representative experiment (Fig. 3, A, B) shows that at 48 h after infection the yield of the
174 recombinants R-87, R-97 and R-99-2 did not significantly differ one from the other, either in SK-
175 OV-3 or in Vero-GCN4R cells. We note that R-LM113 replicated for one passage in wt-Vero cells,
176 and its Vero-GCN4R derivative; however, numerous efforts to passage serially R-LM113 in these
177 cells were unsuccessful, and did not yield any progeny. The two recombinants with lower yields
178 were R-89 and R-99. R-87 and R-89, representative of the best performing and least well

179 performing recombinants, respectively, were further analyzed with respect to the extent of virus
180 release in the extracellular medium. Fig. 3 C, D shows that, for both viruses the extracellular virus
181 yield at 48 h was about 1 log lower than the intracellular virus yield, as was the case for R-LM113.

182 Next, we analyzed the ability of the recombinants to form plaques, with respect to plaque
183 size and plating efficiency. Fig. 4 A shows a typical plaque for each recombinant in Vero-GCN4R
184 and SK-OV-3 cells. The average plaque size of the recombinants is shown in Fig. 4 B. All
185 recombinants formed somewhat larger plaques in Vero-GCN4R than in SK-OV-3 cells. Also with
186 respect to the number of plaques, the efficiency was somewhat higher in the Vero-GCN4R than in
187 the SK-OV-3 (Fig 4 C). Altogether, these results show that the Vero-GCN4R cell line enables
188 efficient spread of the recombinants.

189 In the past, we observed that switching a virus from one cell line to a different cell line for
190 replication may sometime result in a lower replication rate at earliest passages after the switch.
191 Specifically, when a virus is grown in a certain cell line (e.g. Vero-GCN4R) and is then switched to
192 another cell line (e.g. SK-OV-3), there may be a decrease in the efficiency of virus growth at very
193 early passages. We analyzed whether the growth of R-87 and R-97 in Vero-GCN4R cells may
194 affect the extent of replication in the cancer SK-OV-3 cells. R-87 and R-97 were grown in Vero-
195 GCN4R (R-87_{VG} and R-97_{VG}) or in SK-OV-3 cells (R-87_{SK} and R-97_{SK}), and then employed to
196 infect SK-OV-3 cells. Fig. 5 shows that R-87_{VG} grew as efficiently as R-87_{SK} in SK-OV-3 cells.
197 Similarly, R-97_{VG} grew as efficiently as R-97_{SK} in SK-OV-3 cells. Thus, switching from Vero-
198 GCN4R to SK-OV-3 cells exerted no detrimental effect on the efficiency of viral growth.

199

200 **Cell killing ability of double gD retargeted recombinants.** The above candidate oncolytic
201 recombinants were tested for ability to exert cytotoxic activity towards SK-OV-3 and Vero-GCN4R
202 cells. Fig. 6A shows all recombinants were cytotoxic for SK-OV-3 cells. The highest effect was
203 exhibited by the recombinants which replicated better. All the recombinants were cytotoxic also for
204 Vero-GCN4R cells (Fig. 6B). As expected, the exception was R-LM113 in Vero-GCN4R cells,

205 since the virus infects these cells at low efficiency. As noted earlier, the HER2 retargeted viruses
206 infect Vero cells most likely through the simian HER2.

207

208 **Oncolytic efficacy of a double gD retargeted recombinant in immunocompetent mice.**

209 We selected R-87, one of the best performing double gD retargeted recombinants, to evaluate the
210 oncolytic efficacy in immunocompetent mice. The animal model will be described elsewhere in
211 detail under different co-authorship (45). Essentially, it consists of the Lewis lung murine
212 carcinoma 1 (LLC-1) cells made transgenic for human HER2 (hHER2-LLC-1). The cancer cells
213 were implanted in a strain of the syngeneic C57BL6 mice, which are transgenic for, hence tolerant
214 to hHER2. Three days after implantation of the tumor cells, R-87 was administered intratumorally
215 (i.t.) at 3-4 days distance, with 1×10^8 PFU/injection, for a total of 4 treatments. As a comparison
216 we included in the experiment the prototypic R-LM113 and R-317 described in the accompanying
217 paper (46). Fig. 7 A-C shows that the antitumor efficacy of R-87 was very similar to those of R-
218 LM113 and of R-317, and the tumor size was significantly smaller than that in the untreated mice at
219 28 d (Fig. 7 D).

220

221 **DISCUSSION**

222 Recently we developed a system for the cultivation in non-cancer cells of clinical grade oncolytic
223 HSVs retargeted to HER2, and, potentially, to any cancer-specific receptor of choice (39). The
224 potentially universal system is based on a double retargeting strategy. One retargeting is to the
225 cancer receptor, exemplified in our studies by HER2. The other retargeting is by way of the 20 aa
226 long GCN4 peptide, which readdresses the tropism to Vero cells expressing the artificial GCN4R.
227 Here, we asked whether a double retargeting *via* gD is feasible, and whether it can be optimized by
228 means of a less disadvantageous detargeting strategy, designed on the structural analysis of the gD-
229 nectin1 co-crystal (42). We report that gD simultaneously accepts two different heterologous
230 ligands for retargeting to two different receptors. The double retargeting can be combined with
231 novel nectin1-detargeting strategies, based on small deletions at two different loci in gD.

232 Analysis of the panel of gD recombinants shows that all of them were simultaneously
233 retargeted to the GCN4R and to the HER2, and detargeted from both HVEM and nectin1. A novel
234 finding to emerge from this investigation is that the modifications to the locus around aa 214-223 is
235 suitable for nectin1 detargeting, and retargeting. Each of the two heterologous receptors (HER2 and
236 GCN4R) can be used alternatively to the other, and independently of the other. The recombinants
237 switched readily from one cell system (GCN4R-positive cell) to the other (HER2-positive cell).

238 Not all the insertion sites were equivalent, and the combination of ligand to insertion site can
239 be optimized. This conclusion rests on the following examples.

240 Comparison of R-87 *versus* R-97. R-87 and R-97 share the following properties. They carry
241 the same deletion in gD (aa 35-39) for nectin1-detargeting. They carry one of the two inserts (the
242 260 aa long scFv to HER2 or the 20 aa long GCN4 peptide) between aa 24 and 25 for HVEM
243 detargeting. They differ in the relative position of the two inserts. Thus, in R-87 the gD deletion is
244 replaced by the scFv, whereas in R-97 the deletion is replaced by the GCN4 peptide. A comparison
245 of R-87 and R-97 shows that they grew to very similar yields. Hence, exchanging the short GCN4
246 peptide and the scFv at anyone of these two positions was irrelevant with respect to growth capacity.

247 Comparison of R-89 *versus* R-99. R-89 and R-99 share the following properties. They carry
248 the same deletion in gD (aa 214-223) for nectin1-detargeting. They carry one of the two inserts (the
249 scFv to HER2 or the GCN4 peptide) between aa 24 and 25 for HVEM detargeting. They differ in
250 the relative position of the two inserts. Thus, in R-89 the gD deletion is replaced by the scFv,
251 whereas in R-99 the deletion is replaced by the GCN4 peptide. The R-89 and R-99 recombinants
252 replicated in a similar manner, and there was no apparent effect of the relative position of the two
253 inserts. Of note, the yields of R-89 and R-99 were lower than those of R-87 and R-97. Hence, a 10
254 aa deletion at this locus does not enable a highly efficient replication.

255 A comparison of R-97 *versus* R-99-2 sheds light on the effects of performing the deletion in
256 the aa 35-39 locus *versus* the 219-223 locus. At 48 h these two recombinants replicated in a very
257 similar manner in both SK-OV-3 and Vero-GCN4R cells, although a difference was seen at 24 h.
258 Thus, a 5 aa deletion at anyone of these two loci results in very similar recombinants.

259 Comparison of R-99 *versus* R-99-2. These two recombinants differ in that R-99-2 carries a
260 smaller (5 aa) deletion than R-99 (10 aa deletion), and are otherwise identical. The important result
261 here is that R-99-2 grew one log more than R-99, suggesting that the size of the deletion may be
262 critical for a better preservation of gD functions. This may explain why R-87, R-97, and R-99-2,
263 which carry 5 aa long deletions replicated to similar yields. Of note, the differences in virus yield
264 were not fully recapitulated in the plaque size; the latter is influenced not only by virus replication
265 but also by ability to perform cell-to-cell spread.

266 The R-87 recombinant was selected to evaluate the antitumor efficacy *in vivo*, in an
267 immunocompetent mouse model. In general, the murine cancer cells are not as permissive to HSV
268 as the human cancer cells, hence this model underestimates the antitumor efficacy, a property
269 shared with the vast majority of murine cancer models for oncolytic HSVs (47, 48). Here, the
270 important result was that the anti-tumor efficacy of R-87 could not be differentiated from that of R-
271 LM113 and of the gB recombinant R-317, described in the accompanying paper (37). Thus, the
272 replication properties in cell cultures are recapitulated in the *in vivo* anti-tumor efficacy, and a

273 recombinant carrying two retargeting moieties in gD is not at disadvantage relative to R-LM113,
274 which carries a single retargeting moiety. Altogether, the double retargeting *via* gD was feasible.
275 By optimizing the detargeting strategies we generated double-retargeted gD recombinants which
276 replicated as efficiently as the singly retargeted R-LM113 or the non-detargeted R-LM5, and which
277 exerted anti-tumor activity *in vivo* as efficiently as R-LM113.

278 In an accompanying paper, we show that double retargeting is feasible also by insertion of
279 the GCN4 peptide in gB, and of the scFv in gD (46); even in that study (46), a novel gD detargeting
280 strategy was developed. In both studies, the comparison of a number of recombinants lead to
281 optimization of double retargeted recombinants. Together with the previous finding that the double
282 retargeting is achieved by insertion of the GCN4 peptide in gH, and of the scFv to HER2 in gD (39),
283 current data indicate that several alternative strategies have become possible, now that we have
284 enlarged the number of HSV glycoproteins that can serve as retargeting tools, and in the light of
285 accurate knowledge of gD-receptor structures (42). All in all the double gD recombinants and the
286 gB/gD simultaneous retargeting yielded recombinants which replicate at comparable yields and will
287 help move the field of retargeted oncolytic HSVs into the translational phase.

288

289 MATERIALS AND METHODS

290 **Viruses.** R-LM5 and R-LM113 were described (17) (see Table 1, for summary of genotypes
291 and tropism). R-LM5 carries wt-gD ORF, the bacterial artificial chromosome (BAC) sequences
292 cloned in the UL3-UL4 intergenic region, as in the parental pYeBac 102 (49) and the enhanced
293 green fluorescent protein (EGFP) ORF under the $\alpha 27$ promoter cloned within the BAC sequences
294 (17). It is not detargeted/retargeted, therefore is the wt-counterpart of R-LM113, R-87, R-89, R-97,
295 R-99, R-99-2. R-LM113 is identical to R-LM5, except that it carries a HER2-retargeted gD. In
296 particular the deletion of aa 6-38 of mature gD which removes critical residues for interaction with
297 HVEM and nectin1 and its replacement with the scFv to HER2 derived from trastuzumab (44),
298 detargets the virus tropism from the natural receptors. wt HSV-1 F was described (50).

299 **Engineering of R-87, R-89, R-97, R-99, R-99-2.**

300 To engineer the gD double retargeted recombinants we constructed two precursor BAC, BAC 81
301 and BAC 91, starting from LM55 BG BAC. BAC 81 carries GCN4 peptide between aa 24 and 25
302 of gD, whereas BAC 91 carries scFv HER2 in the same position. The HSV-1 recombinants R-87,
303 R-89 were derived from BAC 81 by insertion of the scFv HER2 in place of aa 35-39 (R-87), or in
304 place of aa 214-223 (R-89). The recombinants R-97, R-99, R-99-2 were derived from BAC 91 by
305 insertion of the GCN4 peptide in place of aa 35-39 (R-97), in place of aa 214-223 (R-99), or in
306 place of aa 219-223 (R-99-2). See Fig.1 B and Table 1. The aa sequence of the GCN4 peptide was
307 KNYHLENEVARLKKLG. The core YHLENEVARLKK residues represent the epitope
308 recognized by the single chain antibody C11L34-H6 (PDB # 1P4B) (40). In the recombinant
309 viruses, the GCN4 peptide was preceded and followed by GS linkers. The starting material for the
310 engineering of BAC 81 and BAC 91 was LM55 BG BAC which carries LOX-P-bracketed
311 pBeloBAC11 and eGFP sequences inserted between U_L3 and U_L4 of HSV-1 genome (17). The
312 engineering was performed in bacteria by means of galK recombineering, in two steps (38, 51). In
313 the first step, the galK cassette, with homology arms to gD, was inserted between aa 24 and 25 of
314 mature gD. In the second step, the galK insert was replaced with the GCN4 peptide cassette to

315 generate the precursor BAC 81 or was replaced by the scFv HER2 cassette to generate the precursor
316 BAC 91.

317 To carry out the first step in the engineering of BAC 81, the galK cassette, with homology
318 arms to gD was amplified by means of primers gD24_galK_f and gD25_galK_r (Table 2), using p-
319 galK plasmid as template. The PCR-amplified galK cassette was then electroporated into SW102
320 bacteria, which carry the LM55 BG BAC, to generate BAC 80. To exclude galK false positive
321 colonies, the recombinant clones were plated on Mac Conkey agar base plates, supplemented with
322 1% galactose and 12 µg/ml chloramphenicol, and checked by colony PCR. Colony PCR was carried
323 out with primer galK_827_f and galK_1142_r (Table 2). To carry out the second step and generate
324 the precursor BAC 81, a cassette encoding the GCN4 peptide (GenBank accession number
325 AF416613.1) (40) bracketed by the downstream and upstream Gly-Ser linkers and by homology
326 arms to gD was generated, through annealing and extension of the partially overlapping
327 oligonucleotides gD24_GCN4_fB and gD25_GCN4_rB (Table 2). The oligonucleotides contained
328 a silent BamHI restriction site, for screening purposes. The amplicon encoding the GCN4 cassette,
329 with homology arms to gD, was electroporated into SW102 bacteria carrying BAC 80. The
330 recombinant BAC was named BAC 81. Positive bacterial clones were checked by means of BamHI
331 restriction analysis on colony PCR fragments, amplified with primers gD_ext_f and gD_ext_r
332 (Table 2).

333 The precursor BAC 91 carries the scFv to HER2 between aa 24 to 25 of gD. It was
334 generated from BAC 80. First, the scFv HER2 cassette bracketed by homology arms to gD was
335 amplified by means of primers gD24-scFvHer2-F and gD25-scFvHer2-R (Table 2). Bacterial
336 colonies were checked for the presence of sequence of choice by means of colony PCR with
337 primers gD_ext_f and scFv_456_r (Table 2).

338 To engineer R-87 and R-89, the scFv HER2 was inserted in gD Δ 35-39 (R-87), or in gD
339 Δ 214-223 (R-89), as detailed for BAC 81, by means of oligonucleotides reported in Table 2. To

340 engineer R-97, R-99, and R-99-2, the GCN4 peptide was inserted in gD Δ 35-39 (R-97), gD Δ 214-
341 223 (R-99), or gD Δ 219-223 (R-99-2) of BAC 91, by means of oligonucleotides reported in Table 2.

342 To reconstitute the recombinant viruses, 500 ng of recombinant BAC DNA was transfected
343 into the Vero-GCN4R cell line and SK-OV-3 cell line by means of Lipofectamine 2000 (Life
344 Technologies), and then grown in these cells. Virus growth was monitored by green fluorescence.
345 The structure of the recombinant was verified by sequencing the entire gD. Virus stocks were
346 generated in Vero-GCN4R and SK-OV-3 and titrated in Vero-GCN4R and SK-OV-3 cells. All
347 other recombinants were engineered by the same procedure, by means of oligonucleotides described
348 in Table 2.

349 **Tropism of R-87, R-89, R-97, R-99, R-99-2.** The indicated cells were infected with the
350 indicated viruses at 1 PFU/cell, and monitored 24 h later with a Nikon Eclipse TS100 fluorescence
351 microscope. Where indicated, infection was carried out in the presence of MAb to HER2
352 (trastuzumab) at the concentration of 28 μ g/ml.

353 **Determination of virus growth and extent of viral progeny release.** Vero-GCN4R and
354 SK-OV-3 cells were infected with wt HSV-1 F, R-LM5, R-LM113, R-87, R-89, R-97, R-99, R-99-
355 2 at 0.1 PFU/cell. Unabsorbed virus was inactivated by rinsing the cells with a pH 3 solution (40
356 mM citric acid, 10 mM KCl, 135 mM NaCl). Replicate cultures were frozen at 24 and 48 h after
357 infection. Progeny virus (intracellular plus extracellular) was titrated in SK-OV-3 cells. Results are
358 expressed as the mean of three independent experiments \pm SD. In virus release experiments,
359 replicate cultures of Vero-GCN4R or SK-OV-3 infected with R-LM113, R-87 or R-89 at 0.1
360 PFU/cell were harvested 48 h after infection as cell lysates plus medium. Alternatively medium or
361 cellular fractions were harvested separately. Progeny virus was titrated in SK-OV-3 cells. Results
362 are expressed as the mean of three independent experiments \pm SD.

363 **Plating efficiency and relative plaque size.** Replicate aliquots of R-LM5, R-LM113, R-87,
364 R-89, R-97, R-99, R-99-2 were plated on Vero-GCN4R and SK-OV-3 cells and the number of

365 plaques was counted 3 days later. Results represent the mean of three independent infections \pm SD.
366 For plaque size determination, pictures of 6 individual plaques from each of the above samples
367 were taken 3 days after infection. Plaque areas were measured with Nis Elements-Imaging Software
368 (Nikon). Each result represents areas \pm SD.

369 **Cytotoxicity assay.** SK-OV-3 and Vero-GCN4R cells were seeded in 96 well plates (8×10^3
370 cell/well) and infected with wt HSV-1 F, R-LM5, R-LM113, R-87, R-89, R-97, R-99, R-99-2 (3
371 PFU/cell) or mock-infected. AlamarBlue (10 μ l/well, Life Technologies) was added to the culture
372 media at indicated times after infection and incubated for 4 h at 37°C. Plates were read at 560 and
373 600 nm with GloMax Discover System (Promega Corporation). For each time point, cell viability
374 was expressed as the percentage of alamarBlue reduction in infected versus uninfected cells, after
375 subtraction of the background value (medium alone). Each point represents the average of at least
376 triplicate samples \pm SD.

377 **In vivo anti-tumor efficacy.** C57BL6 mice transgenic for and tolerant to hHER2, received
378 from Jackson Laboratories, were implanted with the murine Lewis lung carcinoma 1 (LLC-1) cells
379 made transgenic for hHER2 (hHER2-LLC-1), 0.2×10^6 cells/mouse (45). Three days later mice
380 received R-87, R-LM113 and R-317 as control viruses, peri-intratumorally (i.t.), four
381 dosages/mouse at 3-4 days distance, 1×10^8 PFU/injection, 5 mice for each treatment group. Tumor
382 size was measured by means of a caliper at the indicated days as described (19). Animal
383 experiments were performed according to European directive 2010/63/UE, Italian laws 116/92 and
384 26/2014. Experimental protocols were reviewed and approved by the University of Bologna Animal
385 Care and Use Committee (“Comitato per il Benessere degli Animali, COBA”), and approved by the
386 Italian Ministry of Health, Authorization # 86/2017-PR to Prof. Anna Zaghini.

387

388 **ACKNOWLEDGMENTS**

389 This work was supported by European Research Council (ERC), Advanced Grant number 340060,
390 by Italian Association for Cancer Research, grant number 14535, to G.C.F and by Fondi Pallotti to
391 Tatiana Gianni.

392 Competing interests. G.C.F. owns shares in Nouscom SRL. B.P. is currently an employee of
393 Nouscom SRL.

394 **FUNDING INFORMATION**

395 EC | European Research Council (ERC) provided funding to Gabriella Campadelli-Fiume under 7th
396 Framework Programme advanced grant number 340060. Italian Association for Cancer Research
397 provided funding to Gabriella Campadelli-Fiume under grant number 14535. The funders had no
398 role in study design, data collection and analysis, decision to publish, or preparation of the
399 manuscript.

400

401 **REFERENCES**

- 402 1. **Coffin RS.** 2015. From virotherapy to oncolytic immunotherapy: where are we now? *Curr*
403 *Opin Virol* **13**:93-100.
- 404 2. **Russell SJ, Peng KW, Bell JC.** 2012. Oncolytic virotherapy. *Nat Biotechnol* **30**:658-670.
- 405 3. **Miest TS, Cattaneo R.** 2014. New viruses for cancer therapy: meeting clinical needs. *Nat*
406 *Rev Microbiol* **12**:23-34.
- 407 4. **Keller BA, Bell JC.** 2016. Oncolytic viruses-immunotherapeutics on the rise. *J Mol Med*
408 (Berl) **94**:979-991.
- 409 5. **Lemay CG, Keller BA, Edge RE, Abei M, Bell JC.** 2017. Oncolytic Viruses: The Best is
410 Yet to Come. *Curr Cancer Drug Targets* doi:10.2174/1568009617666170206111609.
- 411 6. **Andthacka RH, Kaufman HL, Collichio F, Amatruda T, Senzer N, Chesney J, Delman**
412 **KA, Spitler LE, Puzanov I, Agarwala SS, Milhem M, Cranmer L, Curti B, Lewis K,**
413 **Ross M, Guthrie T, Linette GP, Daniels GA, Harrington K, Middleton MR, Miller WH,**
414 **Jr., Zager JS, Ye Y, Yao B, Li A, Doleman S, VanderWalde A, Gansert J, Coffin RS.**
415 2015. Talimogene Laherparepvec Improves Durable Response Rate in Patients With
416 Advanced Melanoma. *J Clin Oncol* doi:10.1200/JCO.2014.58.3377.
- 417 7. **Liu BL, Robinson M, Han ZQ, Branston RH, English C, Reay P, McGrath Y, Thomas**
418 **SK, Thornton M, Bullock P, Love CA, Coffin RS.** 2003. ICP34.5 deleted herpes simplex
419 virus with enhanced oncolytic, immune stimulating, and anti-tumour properties. *Gene Ther*
420 **10**:292-303.
- 421 8. **Chou J, Chen JJ, Gross M, Roizman B.** 1995. Association of a M(r) 90,000
422 phosphoprotein with protein kinase PKR in cells exhibiting enhanced phosphorylation of
423 translation initiation factor eIF-2 alpha and premature shutoff of protein synthesis after
424 infection with gamma 134.5- mutants of herpes simplex virus 1. *Proc Natl Acad Sci U S A*
425 **92**:10516-10520.
- 426 9. **Chou J, Kern ER, Whitley RJ, Roizman B.** 1990. Mapping of herpes simplex virus-1
427 neurovirulence to gamma 134.5, a gene nonessential for growth in culture. *Science*
428 **250**:1262-1266.
- 429 10. **Andreansky S, Soroceanu L, Flotte ER, Chou J, Markert JM, Gillespie GY, Roizman**
430 **B, Whitley RJ.** 1997. Evaluation of genetically engineered herpes simplex viruses as
431 oncolytic agents for human malignant brain tumors. *Cancer Res* **57**:1502-1509.
- 432 11. **Liu TC, Wakimoto H, Martuza RL, Rabkin SD.** 2007. Herpes simplex virus Us3(-)
433 mutant as oncolytic strategy and synergizes with phosphatidylinositol 3-kinase-Akt
434 targeting molecular therapeutics. *Clin Cancer Res* **13**:5897-5902.
- 435 12. **Markert JM, Medlock MD, Rabkin SD, Gillespie GY, Todo T, Hunter WD, Palmer**
436 **CA, Feigenbaum F, Tornatore C, Tufaro F, Martuza RL.** 2000. Conditionally
437 replicating herpes simplex virus mutant, G207 for the treatment of malignant glioma: results
438 of a phase I trial. *Gene Ther* **7**:867-874.
- 439 13. **Zhou G, Roizman B.** 2006. Construction and properties of a herpes simplex virus 1
440 designed to enter cells solely via the IL-13alpha2 receptor. *Proc Natl Acad Sci U S A*
441 **103**:5508-5513.
- 442 14. **Zhou G, Roizman B.** 2007. Separation of receptor binding and pro-fusogenic domains of
443 glycoprotein D of herpes simplex virus 1 into distinct interacting proteins. *Proc Natl Acad*
444 *Sci U S A* **104**:4142-4146.
- 445 15. **Uchida H, Chan J, Goins WF, Grandi P, Kumagai I, Cohen JB, Glorioso JC.** 2010. A
446 double mutation in glycoprotein gB compensates for ineffective gD-dependent initiation of
447 herpes simplex virus type 1 infection. *J Virol* **84**:12200-12209.
- 448 16. **Menotti L, Cerretani A, Campadelli-Fiume G.** 2006. A herpes simplex virus recombinant
449 that exhibits a single-chain antibody to HER2/neu enters cells through the mammary tumor
450 receptor, independently of the gD receptors. *J Virol* **80**:5531-5539.

- 451 17. **Menotti L, Cerretani A, Hengel H, Campadelli-Fiume G.** 2008. Construction of a fully
452 retargeted herpes simplex virus 1 recombinant capable of entering cells solely via human
453 epidermal growth factor receptor 2. *J Virol* **20**:10153-10161.
- 454 18. **Nanni P, Gatta V, Menotti L, De Giovanni C, Ianzano M, Palladini A, Grosso V,
455 Dall'ora M, Croci S, Nicoletti G, Landuzzi L, Iezzi M, Campadelli-Fiume G, Lollini PL.**
456 2013. Preclinical Therapy of Disseminated HER-2(+) Ovarian and Breast Carcinomas with
457 a HER-2-Retargeted Oncolytic Herpesvirus. *PLoS Pathog* **9**:e1003155.
- 458 19. **Menotti L, Nicoletti G, Gatta V, Croci S, Landuzzi L, De Giovanni C, Nanni P, Lollini
459 PL, Campadelli-Fiume G.** 2009. Inhibition of human tumor growth in mice by an
460 oncolytic herpes simplex virus designed to target solely HER-2-positive cells. *Proc Natl
461 Acad Sci USA* **106**:9039-9044.
- 462 20. **Leoni V, Gatta V, Palladini A, Nicoletti G, Ranieri D, Dall'Ora M, Grosso V, Rossi M,
463 Alviano F, Bonsi L, Nanni P, Lollini PL, Campadelli-Fiume G.** 2015. Systemic delivery
464 of HER2-retargeted oncolytic-HSV by mesenchymal stromal cells protects from lung and
465 brain metastases. *Oncotarget*.
- 466 21. **Goins WF, Hall B, Cohen JB, Glorioso JC.** 2016. Retargeting of herpes simplex virus
467 (HSV) vectors. *Curr Opin Virol* **21**:93-101.
- 468 22. **Jackson C, Browell D, Gautrey H, Tyson-Capper A.** 2013. Clinical Significance of HER-
469 2 Splice Variants in Breast Cancer Progression and Drug Resistance. *Int J Cell Biol*
470 **2013**:973584.
- 471 23. **Gu G, Dustin D, Fuqua SA.** 2016. Targeted therapy for breast cancer and molecular
472 mechanisms of resistance to treatment. *Curr Opin Pharmacol* **31**:97-103.
- 473 24. **Campadelli-Fiume G, Amasio M, Avitabile E, Cerretani A, Forghieri C, Gianni T,
474 Menotti L.** 2007. The multipartite system that mediates entry of herpes simplex virus into
475 the cell. *Rev Med Virol* **17**:313-326.
- 476 25. **Campadelli-Fiume G, Menotti L, Avitabile E, Gianni T.** 2012. Viral and cellular
477 contributions to herpes simplex virus entry into the cell. *Curr Opin Virol* **2**:28-36.
- 478 26. **Connolly SA, Jackson JO, Jardetzky TS, Longnecker R.** 2011. Fusing structure and
479 function: a structural view of the herpesvirus entry machinery. *Nat Rev Microbiol* **9**:369-
480 381.
- 481 27. **Heldwein EE, Krummenacher C.** 2008. Entry of herpesviruses into mammalian cells. *Cell
482 Mol Life Sci* **65**:1653-1668.
- 483 28. **Eisenberg RJ, Atanasiu D, Cairns TM, Gallagher JR, Krummenacher C, Cohen GH.**
484 2012. Herpes virus fusion and entry: a story with many characters. *Viruses* **4**:800-832.
- 485 29. **Sathiyamoorthy K, Chen J, Longnecker R, Jardetzky TS.** 2017. The COMPLEXity in
486 herpesvirus entry. *Curr Opin Virol* **24**:97-104.
- 487 30. **Cocchi F, Lopez M, Menotti L, Aoubala M, Dubreuil P, Campadelli-Fiume G.** 1998.
488 The V domain of herpesvirus Ig-like receptor (HIgR) contains a major functional region in
489 herpes simplex virus-1 entry into cells and interacts physically with the viral glycoprotein D.
490 *Proc Natl Acad Sci U S A* **95**:15700-15705.
- 491 31. **Geraghty RJ, Krummenacher C, Cohen GH, Eisenberg RJ, Spear PG.** 1998. Entry of
492 alphaherpesviruses mediated by poliovirus receptor-related protein 1 and poliovirus receptor.
493 *Science* **280**:1618-1620.
- 494 32. **Carfi A, Willis SH, Whitbeck JC, Krummenacher C, Cohen GH, Eisenberg RJ, Wiley
495 DC.** 2001. Herpes simplex virus glycoprotein D bound to the human receptor HveA. *Mol
496 Cell* **8**:169-179.
- 497 33. **Chowdary TK, Cairns TM, Atanasiu D, Cohen GH, Eisenberg RJ, Heldwein EE.** 2010.
498 Crystal structure of the conserved herpesvirus fusion regulator complex gH-gL. *Nat Struct
499 Mol Biol* **17**:882-888.

- 500 34. **Gianni T, Salvioli S, Chesnokova LS, Hutt-Fletcher LM, Campadelli-Fiume G.** 2013.
501 alphavbeta6- and alphavbeta8-integrins serve as interchangeable receptors for HSV gH/gL
502 to promote endocytosis and activation of membrane fusion. *PLoS Pathog* **9**:e1003806.
- 503 35. **Gianni T, Massaro R, Campadelli-Fiume G.** 2015. Dissociation of HSV gL from gH by
504 alphavbeta6- or alphavbeta8-integrin promotes gH activation and virus entry. *Proc Natl*
505 *Acad Sci U S A* **112**:E3901-3910.
- 506 36. **Heldwein EE, Lou H, Bender FC, Cohen GH, Eisenberg RJ, Harrison SC.** 2006.
507 Crystal structure of glycoprotein B from herpes simplex virus 1. *Science* **313**:217-220.
- 508 37. **Petrovic B, Gianni T, Gatta V, Campadelli-Fiume G.** 2017. Insertion of a ligand to
509 HER2 in gB retargets HSV tropism and obviates the need for activation of the other entry
510 glycoproteins. *PLoS Pathog* **13**:e1006352.
- 511 38. **Gatta V, Petrovic B, Campadelli-Fiume G.** 2015. The Engineering of a Novel Ligand in
512 gH Confers to HSV an Expanded Tropism Independent of gD Activation by Its Receptors.
513 *PLoS Pathog* **11**:e1004907.
- 514 39. **Leoni V, Gatta V, Casiraghi C, Nicosia A, Petrovic B, Campadelli-Fiume G.** 2017. A
515 Strategy for Cultivation of Retargeted Oncolytic Herpes Simplex Viruses in Non-cancer
516 Cells. *J Virol* **91**.
- 517 40. **Zahnd C, Spinelli S, Luginbuhl B, Amstutz P, Cambillau C, Pluckthun A.** 2004.
518 Directed in vitro evolution and crystallographic analysis of a peptide-binding single chain
519 antibody fragment (scFv) with low picomolar affinity. *J Biol Chem* **279**:18870-18877.
- 520 41. **Nakamura T, Peng KW, Harvey M, Greiner S, Lorimer IA, James CD, Russell SJ.**
521 2005. Rescue and propagation of fully retargeted oncolytic measles viruses. *Nat Biotechnol*
522 **23**:209-214.
- 523 42. **Di Giovine P, Settembre EC, Bhargava AK, Luftig MA, Lou H, Cohen GH, Eisenberg**
524 **RJ, Krummenacher C, Carfi A.** 2011. Structure of herpes simplex virus glycoprotein d
525 bound to the human receptor nectin-1. *PLoS Pathog* **7**:e1002277.
- 526 43. **Cocchi F, Menotti L, Mirandola P, Lopez M, Campadelli-Fiume G.** 1998. The
527 ectodomain of a novel member of the immunoglobulin subfamily related to the poliovirus
528 receptor has the attributes of a bona fide receptor for herpes simplex virus types 1 and 2 in
529 human cells. *J Virol* **72**:9992-10002.
- 530 44. **Kubetzko S, Balic E, Waibel R, Zangemeister-Wittke U, Pluckthun A.** 2006.
531 PEGylation and multimerization of the anti-p185HER-2 single chain Fv fragment 4D5:
532 effects on tumor targeting. *J Biol Chem* **281**:35186-35201.
- 533 45. **Leoni V, Gatta V, Casiraghi C, Vannini A, Zaghini A, Rambaldi J, Barboni C, Lollini**
534 **P-L, Nanni P, Campadelli-Fiume G.** 2017. A fully virulent HER2-retargeted oncolytic
535 HSV armed with IL12 exerts potent antitumor activity towards distal untreated tumors.
536 Manuscript in preparation
- 537 46. **Petrovic B, Leoni V, Gatta V, Vannini A, Campadelli-Fiume G.** 2017. Dual ligand
538 insertion in gB and in gD of oncolytic HSVs for the retargeting to a producer Vero cell line
539 and to cancer cells. *Journal of Virology* **submitted**.
- 540 47. **Moesta AK, Cooke K, Piasecki J, Mitchell P, Rottman JB, Fitzgerald K, Zhan J, Yang**
541 **B, Le T, Belmontes B, Ikotun OF, Merriam K, Glaus C, Ganley K, Cordover DH,**
542 **Boden AM, Ponce R, Beers C, Beltran PJ.** 2017. Local Delivery of OncoVEXmGM-CSF
543 Generates Systemic Antitumor Immune Responses Enhanced by Cytotoxic T-Lymphocyte-
544 Associated Protein Blockade. *Clin Cancer Res* **23**:6190-6202.
- 545 48. **Hutzen B, Chen CY, Wang PY, Sprague L, Swain HM, Love J, Conner J, Boon L,**
546 **Cripe TP.** 2017. TGF-beta Inhibition Improves Oncolytic Herpes Viroimmunotherapy in
547 Murine Models of Rhabdomyosarcoma. *Mol Ther Oncolytics* **7**:17-26.
- 548 49. **Tanaka M, Kagawa H, Yamanashi Y, Sata T, Kawaguchi Y.** 2003. Construction of an
549 excisable bacterial artificial chromosome containing a full-length infectious clone of herpes

- 550 simplex virus type 1: viruses reconstituted from the clone exhibit wild-type properties in
551 vitro and in vivo. *J Virol* **77**:1382-1391.
- 552 50. **Ejercito PM, Kieff ED, Roizman B.** 1968. Characterization of herpes simplex virus strains
553 differing in their effects on social behaviour of infected cells. *J Gen Virol* **2**:357-364.
- 554 51. **Warming S, Costantino N, Court DL, Jenkins NA, Copeland NG.** 2005. Simple and
555 highly efficient BAC recombineering using galK selection. *Nucleic Acids Res* **33**:e36.
556
- 557

558 **FIGURE LEGENDS**

559 **Fig. 1.** Genome arrangement of recombinants generated in this study. (A) Prototypic genome
560 arrangement of recombinants. Each recombinant carries the BAC sequence and the $\alpha 27$ -promoter
561 driven EGFP (enhanced green fluorescence protein), bracketed by LoxP sites, cloned in the UL3
562 and UL4 intergenic region, the GCN4 peptide and the scFv to HER2 in appropriate sites of gD as
563 detailed below. The Unique Long (UL) and Unique Short (US) portions of the genome, bracketed
564 by terminal (TR) and internal repeats (IR), along with the location of gB and gH genes are shown.
565 (B) Specific genotypic modifications in gD gene of each recombinant.

566

567 **Fig. 2.** Tropism of R-87, R-89, R-97, R-99, and R-99-2 recombinants, and, for comparison, of R-
568 LM113 in the indicated cell lines. (A-F) The indicated cells were infected with R-87 (A), R-89 (B),
569 R-97 (C), R-99 (D), R-99-2 (E) and for comparison, R-LM113 (F) at an MOI of 1 PFU/cell and
570 monitored for EGFP expression by fluorescence microscopy 24 h post infection. J-cells express no
571 receptor for wt HSV; J-HER2, J-nectin1, and J-HVEM express the indicated receptor. Infection was
572 carried out in the absence of antibodies (no Ab), or in the presence of the humanized anti-HER2
573 monoclonal antibody trastuzumab at a concentration of 28 $\mu\text{g/ml}$. (G-H) Tropism of R-87 (G) and
574 R-99 (H) recombinants grown in Vero-GCN4R cell. Cells were infected and monitored for EGFP
575 expression as described above. The panels were adjusted by means of Adobe Photoshop software to
576 match one to the other in the final gallery. The level, brightness and contrast of each panel were
577 adjusted as follow R-87 (A) panels a,b,c,f +35 +75 +100, panels d,e,g,h,i,j,k +35 +25 +100; R-89
578 (B) panels a,b,e,f +35 +75 +100, panels c,g +35 +75 0, panels d,h,i,j,k +35 +25 +100; R-97 (C)
579 panels a,b,e,f,g +35 +75 +100, panel c +35 +75 0, panels d,h +35 +25 0, panels i,j,k +35 +25 +100;
580 R-99 (D) panels a,c,g +35 +75 0, panels b,e,f +35 +75 +100, panels d,h +35 +25 0, panels i,j,k +35
581 +25 +100; R-99-2 (E) panels a,b,e,f +35 +75 +100, panels c,g +35 +75 0, panels d,h,i,j,k +35 +25
582 +100; R-LM113 (F) panels a,b,e,f +35 +75 +100, panels c,g +35 +75 0, panels d,h,i,j,k +35 +25
583 +100. R-87_{VG} (G) panels a,b +50 +75 +100, panel c +35 +100 +0, panels d,e,f,g +50 +25 +100,

584 panels h,i,j,k +50 0 +100; R-99_{VG} (H) panels a,b,e,f +35 +75 +100, panel c +35 +75 0, panels
 585 d,h,i,j,k +35 +25 +100, panel g +15 +75 0

586

587 **Fig. 3.** Yield of R-87, R-89, R-97, R-99, and R-99-2 recombinants, and of R-LM5, R-LM113 and
 588 wt-HSV-1(F), for comparison. (A, B) SK-OV-3 (A) and Vero-GCN4R (B) cells were infected with
 589 the indicated viruses at 0.1 PFU/cell. Progeny virus collected at 24 or 48 h after infection was
 590 titrated in SK-OV-3 cells. Results represent the average of triplicates, \pm SD. (C, D) Production of
 591 intracellular and extracellular R-87, R-89, and R-LM113 in SK-OV-3 (C) and in Vero-GCN4R (D)
 592 cells. Replicate cultures were infected as above. At 48 h after infection, media (extra) and cells
 593 (intra) were harvested separately, or together (intra + extra). Progeny virus was titrated in SK-OV-3
 594 cells. Results represent the average of triplicates, \pm SD.

595

596 **Fig. 4.** Plating efficiency of the indicated recombinants in Vero-GCN4R and SK-OV-3 cells. (A) A
 597 typical plaque is shown for each virus in the indicated cells. (B) Average plaque size of the
 598 indicated recombinants in Vero-GCN4R and SK-OV-3 cells. Six pictures were taken for each
 599 recombinants. Plaque areas were measured with Nis Elements-Imaging software (Nikon). (C)
 600 Replicate aliquots of viruses were plated in SK-OV-3 and Vero-GCN4R cells. Plaques were scored
 601 three days later. The relative number of plaques formed by each virus in the indicated cell line is
 602 reported as percentage of the number of plaques formed in SK-OV-3 cells. Results represent the
 603 average of triplicates, \pm SD. The panels were adjusted by means of Adobe Photoshop software to
 604 match one to the other in the final gallery. The level, brightness and contrast of each panel were
 605 adjusted as follow. Panel a +30 +50 +100, panels b,h,n +20 +50 +100, panels c,d,k,l +50 +25 +50,
 606 panels e,f +35 +20 +100, panel g +35 +50 +100, panels i,j +35 +25 +100, panel m +30 +75 +100.

607

608 **Fig. 5.** Comparative yield of R-87 and R-97 pre-cultivated in SK-OV-3 or Vero-GCN4R cells. R-87
 609 and R-97 were cultivated in SK-OV-3 (R-87_{SK}, R-97_{SK}) or in Vero-GCN4R (R-87_{VG}, R-97_{VG}) cells

610 and employed to infect SK-OV-3 cells at 0.1 PFU/cell. Progeny virus harvested at 24 or 48 h after
611 infection was titrated in SK.OV-3 cells. Results represent the average of triplicates, \pm SD.

612

613 **Fig. 6.** Cell killing ability of the indicated viruses for SK-OV-3 and Vero-GCN4R cells. (A, B) SK-
614 OV-3 (A) or Vero-GCN4R (B) cells were infected with the indicated recombinants, or with HSV-
615 1(F), R-LM5, or R-LM113 as controls, at 3 PFU/cell. Cell viability was quantified by alamarBlue
616 assay at the indicated days after infection. Results represent a typical experiment; each sample is the
617 average of triplicate assay \pm SD.

618

619 **Fig. 7.** Antitumor activity of R-87. A-C. Groups of 5 mice from the hHER2-transgenic C57BL6
620 strain were implanted with hHER2-LLC-1 cells (0.2×10^6 cell) in the left flank. Starting 3 d later,
621 mice received four intratumoral treatments with the indicated viruses, at 3-4 d distance, 1×10^8
622 PFU/treatment.. Tumor volumes for each treatment group are shown. D. Distribution of the tumor
623 size at 28 d after the initial treatment. This experiment is the same as that shown in Fig. 6 of the
624 accompanying paper (37).

625

626 Table 1. Summary of genotypes and major phenotypic properties of the listed recombinants

Recombinant HSV-1	GCN4 position in gD	scFv-HER2 position in gD	Retargeting to HER2	Detargeting from nectin1/HVEM	Ref
R-87	24-25	Δ35-39	+	+	This paper
R-89	24-25	Δ214-223	+	+	This paper
R-97	Δ35-39	24-25	+	+	This paper
R-99	Δ214-223	24-25	+	+	This paper
R-99-2	Δ219-223	24-25	+	+	This paper
R-LM113	none	Δ6-38	+	+	(17)
R-LM5	none	no scFv, no deletion	-	-	(17)

627

628 Table 2. Oligonucleotides employed to engineer the indicated recombinants.

BAC-81	GCN4 peptide cassette inserted between aa 24 and 25 of mature gD of LM55 BAC
1) galK insertion in gD 24-25	Forward: gD24_galK_f CTC TCA AGA TGG CCG ACC CCA ATC GCT TTC GCG GCA AAG ACC TTC CGG TCC CTG TTG ACA ATT AAT CAT CGG CA Reverse: gD25_galK_r TGG ATG TGG TAC ACG CGC CGG ACC CCC GGA GGG TCG GTC AGC TGG TCC AGT CAG CAC TGT CCT GCT CCT T
2) colony PCR for screening	Forward: galK_827_f GCG TGA TGT CAC CAT TGA AG Reverse: galK_1142_r TAT TGT TCA GCG ACA GCT TG
3) GCN4 cassette insertion in place of galK	Forward: gD24_GCIN4_fB CTC TCA AGA TGG CCG ACC CCA ATC GCT TTC GCG GCA AAG ACC TTC CGG TCG GAT CCA AGA ACT ACC ACC TGG AGA ACG AGG TGG CCA GAC TGA AGA AGC TGG TGG GCA GC Reverse: gD25_GCIN4_rB TGG ATG TGG TAC ACG CGC CGG ACC CCC GGA GGG TCG GTC AGC TGG TCC AGG CTG CCC ACC AGC TTC TTC AGT CTG GCC ACC TCG TTC TCC AGG TGG TAG TTC TTG GAT CC
4) colony PCR for screening	Forward: gD_ext_f TCC ATA CCG ACC ACA CCG ACG AAT CCC Reverse: gD_ext_r GAG TTT GAT ACC AGA CTG ACC GTG
R-87	scFv HER2 inserted in gD Δ35-39 of BAC 81
1) galK insertion in gD Δ35-39	Forward: galK_gD35_F TGA AGA AGC TGG TGG GCA GCC TGG ACC AGC TGA CCG ACC CTC CGG GGG TCC CTG TTG ACA ATT AAT CAT CGG CA Reverse: galK_gD39_R GTG ATC GGG AGG CTG GGG GGC TGG AAC GGG TCT GGT AGG CCC GCC TGG ATT CAG CAC TGT CCT GCT CCT T
2) scFv HER2 insertion in place of galK	Forward: gD-34-scFvHER2-F TGA AGA AGC TGG TGG GCA GCC TGG ACC AGC TGA CCG ACC CTC CGG GGG TCG AGA ATT CCG ATA TCC AGA T Reverse: gD-40-scFvHER2-R GTG ATC GGG AGG CTG GGG GGC TGG AAC GGG TCT GGT AGG CCC GCC TGG ATG GAT CCA CCG GAA CCA GAG C
3) colony PCR for screening	Forward: gD_ext_f TCC ATA CCG ACC ACA CCG ACG AAT CCC Reverse: scFv_456_r AGC TGC ACA GGA CAA ACG GAG TGA GCC CCC
R-89	scFv HER2 inserted in gD Δ214-223 of BAC 81

1) galK insertion in gD Δ214-223	Forward: galK_gD214_F CCT ACC AGC AGG GGG TGA CGG TGG ACA GCA TCG GGA TGC TGC CCC GCT TCC CTG TTG ACA ATT AAT CAT CGG CA Reverse: galK_gD223_R CTC GTG TAT GGG GCC TTG GGC CCG TGC CAC CCG GCG ATC TTC AAG CTG TAT CAG CAC TGT CCT GCT CCT T
2) scFv HER2 insertion in place of galK	Forward: gD213-scFvHER2f CCT ACC AGC AGG GGG TGA CGG TGG ACA GCA TCG GGA TGC TGC CCC GCT TCG AGA ATT CCG ATA TCC AGA T Reverse: gD224-scFvHER2r CTC GTG TAT GGG GCC TTG GGC CCG TGC CAC CCG GCG ATC TTC AAG CTG TAG GAT CCA CCG GAA CCA GAG C
3) colony PCR for screening	Forward: gDintforw CCC TAC AAC CTG ACC ATC GCT TGG Reverse: scFv_456_r AGC TGC ACA GGA CAA ACG GAG TGA GCC CCC
BAC 91	scFv HER2 cassette inserted between aa 24 and 25 of mature gD of LM55 BAC
1) scFv HER2 insertion in place of galK	Forward: gD24-scFvHer2-F CTC TCA AGA TGG CCG ACC CCA ATC GCT TTC GCG GCA AAG ACC TTC CGG TCG AGA ATT CCG ATA TCC AGA TG Reverse: gD25-scFvHer2-R TGG ATG TGG TAC ACG CGC CGG ACC CCC GGA GGG TCG GTC AGC TGG TCC AGG GAT CCA CCG GAA CCA GAG C
2) Colony PCR for screening	Forward: gD_ext_f TCC ATA CCG ACC ACA CCG ACG AAT CCC Reverse: scFv_456_r AGC TGC ACA GGA CAA ACG GAG TGA GCC CCC
R-97	GCN4 inserted in gD Δ35-39 of BAC 91
1) galK insertion in gD Δ35-39	Forward: gD35-galK-F GCT CTG GTT CCG GTg GaT CCC TGG ACC AGC TGA CCG ACC CTC CGG GGG TCC CTG TTG ACA ATT AAT CAT CGG CA Reverse: gD39-galK-R GTG ATC GGG AGG CTG GGG GGC TGG AAC GGG TCT GGT AGG CCC GCC TGG ATT CAG CAC TGT CCT GCT CCT T
2) GCN4 insertion in place of galK	Forward: gD35-GCN4-F GCT CTG GTT CCG GTg GaT CCC TGG ACC AGC TGA CCG ACC CTC CGG GGG TCG GAT CCA AGA ACT ACC ACC TGG AGA ACG AGG TGG CCA GAC TGA AGA AGC TGG TGG GCA GC Reverse: gD39-GCN4-R GTG ATC GGG AGG CTG GGG GGC TGG AAC GGG TCT GGT AGG CCC GCC TGG ATG CTG CCC ACC AGC TTC TTC AGT CTG GCC ACC TCG TTC TCC AGG TGG TAG TTC TTG GAT CC
3) colony PCR for screening	Forward: scFv4D5 651_f GGA CAC TGC CGT CTA TTA TTG TAG CCG CT Reverse: gDintrev CCA GTC GTT TAT CTT CAC GAG CCG
R-99	GCN4 inserted in gD Δ214-223 of BAC 91
1) galK insertion in gD Δ214-223	Forward: galK_gD214_F CCT ACC AGC AGG GGG TGA CGG TGG ACA GCA TCG GGA TGC TGC CCC GCT TCC CTG TTG ACA ATT AAT CAT CGG CA Reverse: galK_gD223_R CTC GTG TAT GGG GCC TTG GGC CCG TGC CAC CCG GCG ATC TTC AAG CTG TAT CAG CAC TGT CCT GCT CCT T
2) GCN4 insertion in place of galK	Forward: gD213-GCN4-F CCT ACC AGC AGG GGG TGA CGG TGG ACA GCA TCG GGA TGC TGC CCC GCT TCG GAT CCA AGA ACT ACC ACC TGG AGA ACG AGG TGG CCA GAC TGA AGA AGC TGG TGG GCA GC Reverse: gD224-GCN4-R CTC GTG TAT GGG GCC TTG GGC CCG TGC CAC CCG GCG ATC TTC AAG CTG TAG CTG CCC ACC AGC TTC TTC AGT CTG GCC ACC TCG TTC TCC AGG TGG TAG TTC TTG GAT CC
3) Colony PCR for screening	Forward: gDintforw CCC TAC AAC CTG ACC ATC GCT TGG Reverse: HSV_139688_r CCG ACT TAT CGA CTG TCC ACC TTT CCC

screening	
R-99-2	GCN4 inserted in gD Δ219-223 of BAC 91
1) galK insertion in gD Δ214-223	Forward: galK_gD214_F CCT ACC AGC AGG GGG TGA CGG TGG ACA GCA TCG GGA TGC TGC CCC GCT TCC CTG TTG ACA ATT AAT CAT CGG CA Reverse: galK_gD223_R CTC GTG TAT GGG GCC TTG GGC CCG TGC CAC CCG GCG ATC TTC AAG CTG TAT CAG CAC TGT CCT GCT CCT T
2) GCN4 insertion in place of galK	Forward: gD219-GCN4-F CCT ACC AGC AGG GGG TGA CGG TGG ACA GCA TCG GGA TGC TGC CCC GCT TCA TCC CCG AGA ACC AGC GCG GAT CCA AGA ACT ACC ACC TGG AGA ACG AGG TGG CCA GAC TGA AGA AGC TGG Reverse: gD224-GCN4-R CTC GTG TAT GGG GCC TTG GGC CCG TGC CAC CCG GCG ATC TTC AAG CTG TAG CTG CCC ACC AGC TTC TTC AGT CTG GCC ACC TCG TTC TCC AGG TGG TAG TTC TTG GAT CC
3) colony PCR for screening	Forward: gDintforw CCC TAC AAC CTG ACC ATC GCT TGG Reverse: HSV_139688_r CCG ACT TAT CGA CTG TCC ACC TTT CCC

629

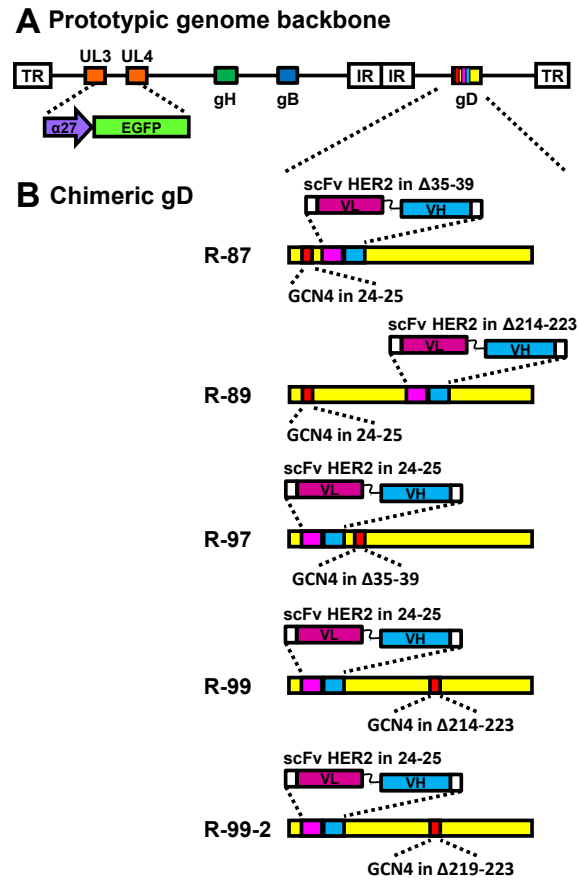


Figure 1

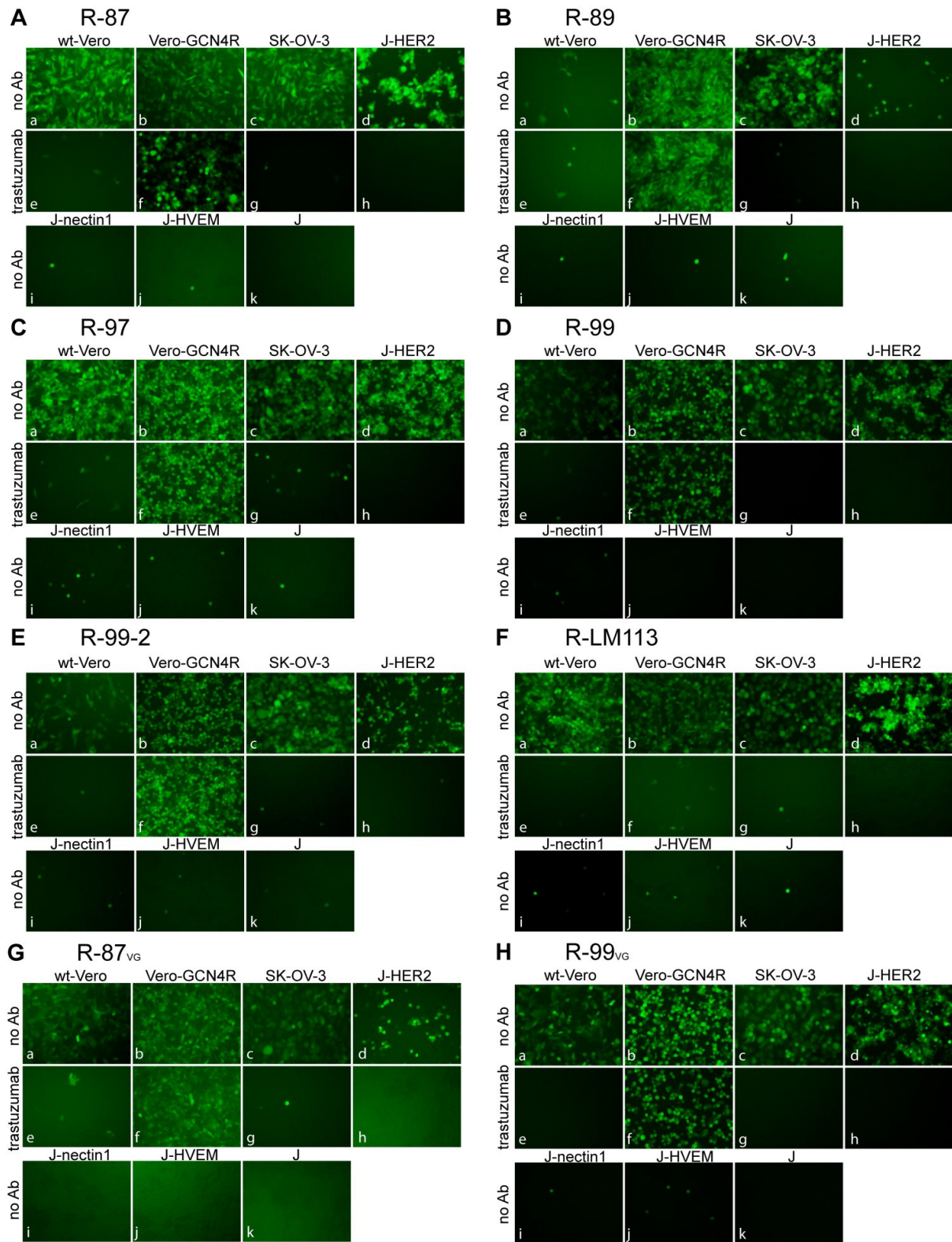


Figure 2

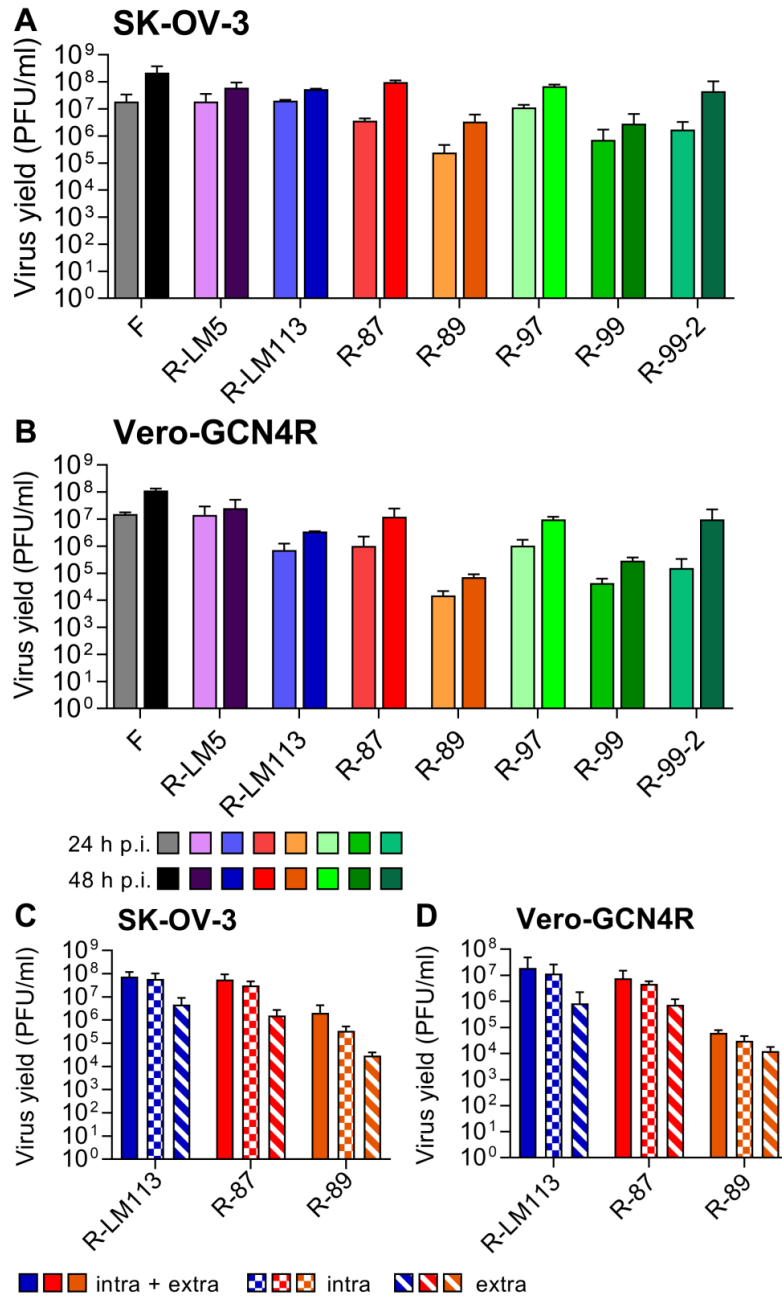


Figure 3

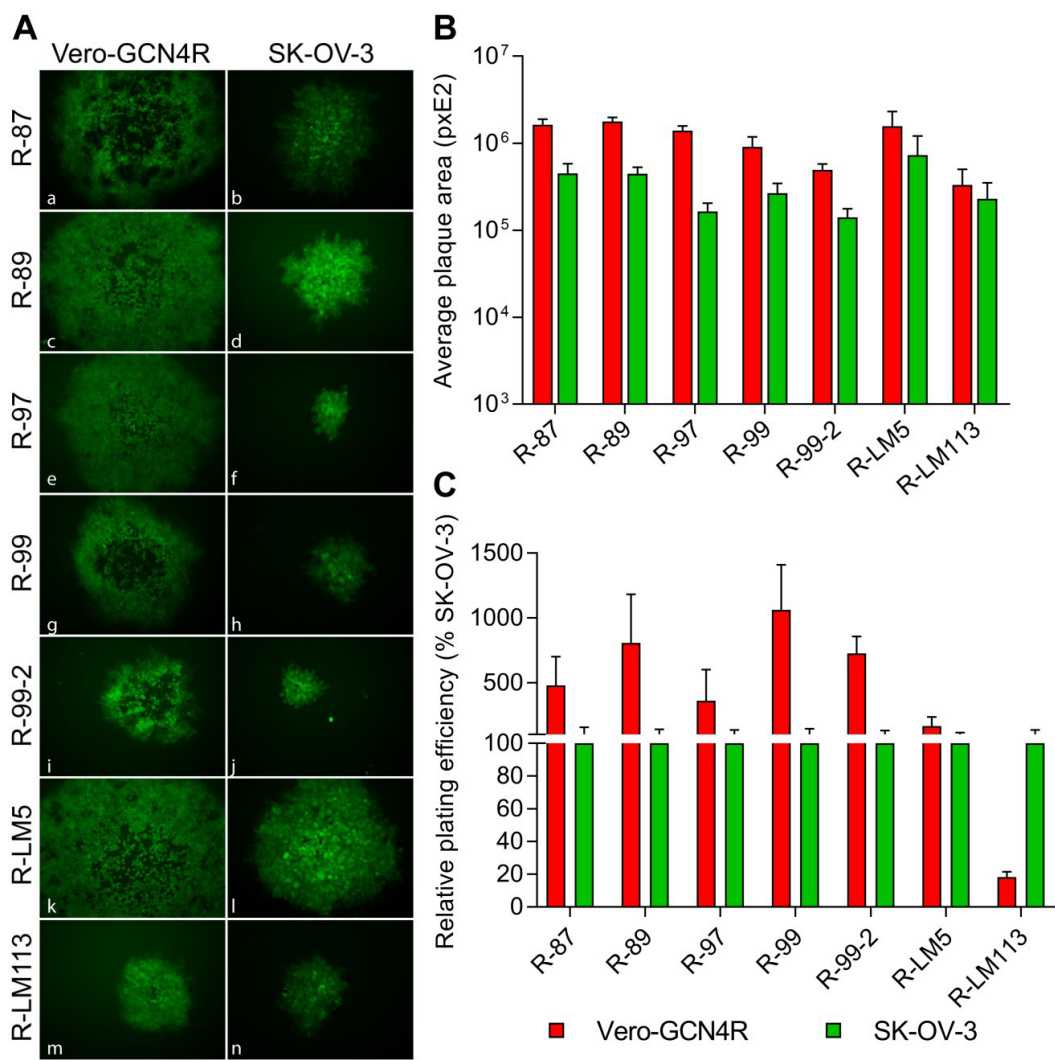


Figure 4

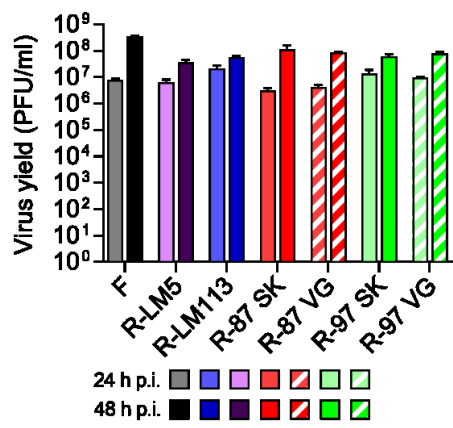


Figure 5

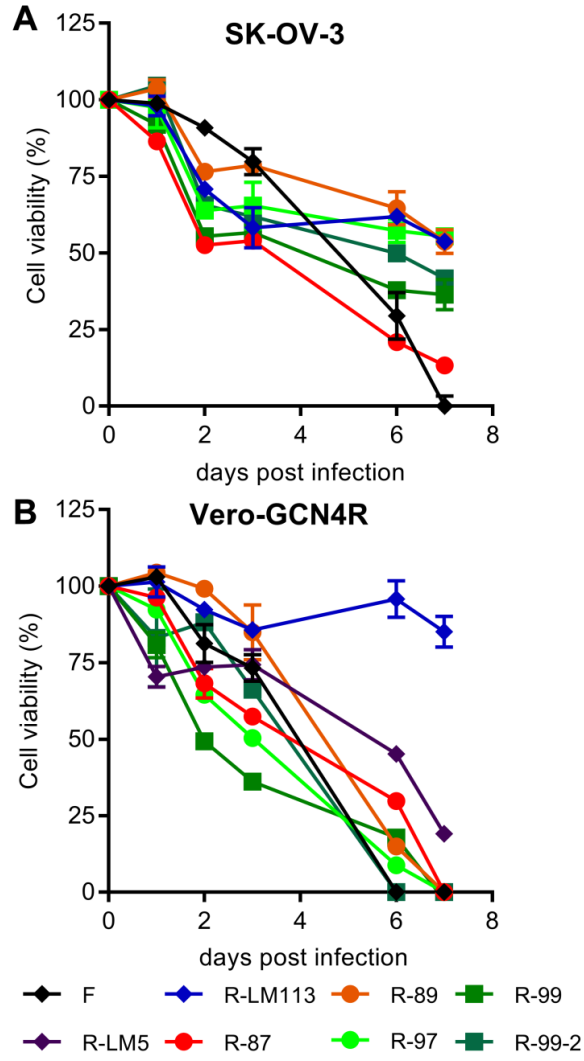


Figure 6

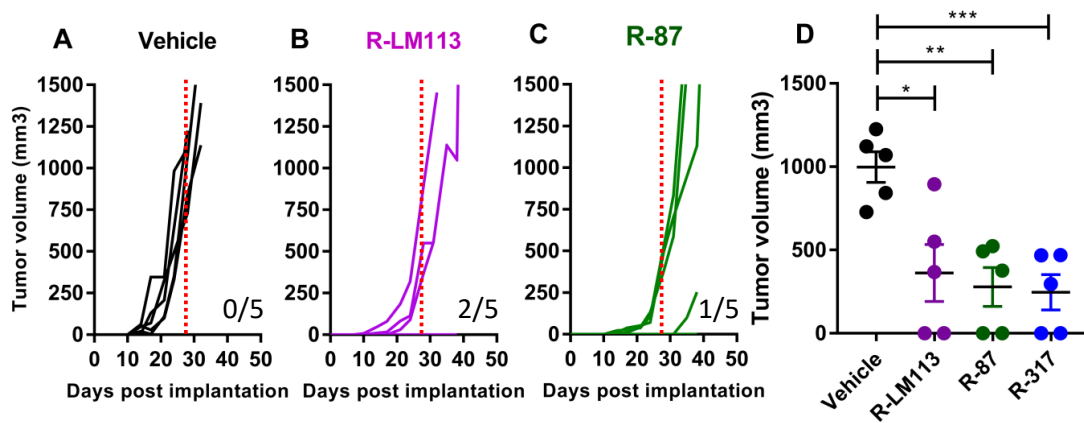


Figure 7